Convergence of Neural Systems Processing Stimulus Associations and Coordinating Motor Responses

A.R. McIntosh, N.J. Lobaugh, R. Cabeza[1], F.L. Bookstein[2] and S.Houle[3]

Rotman Research Institute of Baycrest Centre, Toronto, [1]Department of Psychology, University of Alberta, Canada, [2]Institute of Gerontology, University of Michigan, Ann Arbor, MI, USA and [3]PET Centre, Clarke Institute of Psychiatry; University of Toronto, Ontario, Canada

A sensory–sensory learning paradigm was used to measure neural changes in humans during acquisition of an association between an auditory and visual stimulus. Three multivariate partial least-squares (PLS) analyses of positron emission tomography data identified distributed neural systems related to (i) processing the significance of the auditory stimulus, (ii) mediating the acquisition of the behavioral response, and (iii) the spatial overlap between these two systems. The system that processed the significance of the tone engaged primarily right hemisphere regions and included dorsolateral prefrontal cortex, putamen, and inferior parietal and temporal cortices. Activity changes in left occipital cortex were also identified, most likely reflecting the learned expectancy of the upcoming visual event. The system related to behavior was similar to that which coded the significance of the tone, including dorsal occipital cortex. The PLS analysis of the concordance between these two systems showed substantial regional overlap, and included occipital, dorsolateral prefrontal, and limbic cortices. However, activity in dorsomedial prefrontal cortex was strictly related to processing the auditory stimulus and not to behavior. Taken together, the PLS analyses identified a system that contained a sensory-motor component (comprised of occipital, temporal association and sensorimotor cortices) and a medial prefrontal-limbic component, that as a group simultaneously embodied the learning-related response to the stimuli and the subsequent change in behavior.

Introduction

The study of the relationships between stimulus and response factors in associative learning has a rich behavioral history (Bower and Hilgard, 1981; Domjan and Burkhard, 1982). Converging evidence across a number of behavioral studies suggests basic mechanisms are used across species in the acquisition of information about stimulus–stimulus relations, which interact with, and modify, responses. Some significant strides towards understanding the neural basis of associative learning have also been made. A central role for the cerebellum and cerebellar nuclei in certain forms of classical conditioning has been established (Lavond et al., 1993; Molchan et al., 1994; Logan and Grafton, 1995; Blaxton et al., 1996; Schreurs et al., 1997). The hippocampal formation, though usually associated with aspects of explicit memory, appears to serve some key role in more complex classical and operant conditioning paradigms (Sutherland and Rudy, 1989; Daum et al., 1992; Channon et al., 1993). A large body of work has demonstrated that sensory systems are sensitive to the relations of stimuli to behavior and adapt to the changing meaning of stimuli in the world (Weinberger and Diamond, 1987; Bakin and Weinberger, 1990; Gonzalez-Lima, 1992; Recanzone et al., 1992; Molchan et al., 1994). On the motor output side, several researchers have observed modulation of motor system activity as a new response is acquired (Seitz et al., 1990; Aizawa et al., 1991; Grafton et al., 1992; Jenkins et al., 1994; Karni et al., 1995). Taken together, a number of brain areas have been identified that can code temporospatial relations among stimulus events, in addition to areas associated with modifying behavioral output in learning tasks. Most of the previous work has emphasized one of these domains (stimulus–stimulus associations or responses). In the present study, we combined these two emphases to determine whether there is convergence between the neural systems that process the stimulus significance and those engaged in modifying behavioral responses.

To answer this question, we studied the neural effects of sensory–sensory associative learning. In the present task, an auditory stimulus came to predict the onset of two visual stimuli. To provide an objective measure of acquisition, a button press to one of the two visual stimuli was required. As there was a temporal relation between the auditory and visual stimuli, the expectation was that subjects would learn this association, and show progressively faster reaction times on trials where the auditory stimulus preceded a visual target. We expected to see this learning reflected in a changed neural response to the tone as the association was learned. Positron emission tomography (PET) regional cerebral blood flow (rCBF) was used to measure distributed patterns of functional brain activity. The issues we examined were whether there were patterns of activity most related to: (i) the change in the neural response to the tone as it acquired associative strength; (ii) the behavioral change as the stimulus–stimulus association was learned. Finally, we examined the extent of the overlap between these two patterns.

Materials and Methods

Subjects

Ten adults (mean age 25 years, six females) were recruited from the University of Toronto community. Prior to participation, subjects were screened to ensure none suffered from medical, neurological or psychiatric disorders, and gave written informed consent before participating in the study; they were paid for participation. The Human Subjects Use Committee of Baycrest Centre approved the experimental protocol at the University of Toronto.

PET Scans

PET scans were obtained using a protocol presented elsewhere (Nyberg et al., 1996b; Cabeza et al., 1997). Six PET scans were conducted following a bolus injections of 40 mCi [^{15}O]H$_2$O for each scan. Images were acquired over 60 s using a GEMS-Scanditronix PC2048-15B head scanner (in-plane resolution 5–6 mm) and measurements began when the bolus tracer arrived in the head. The interscan interval was 11 min. Radioactive counts were used as an indirect indication of rCBF (Herscovitch et al., 1983).

Stimuli and Task

Stimuli

Visual stimuli were presented on a computer screen mounted ~60 cm from the subject's face. Two highly discriminable visual stimuli were

used: a circle made of thick concentric lines (target) and one made of thin lines (distractor, see Fig. 1*a*). The outer diameter of the circles was 13 cm, so the stimuli subtended ~13° of visual angle. A fixation cross (2 × 2 cm) was displayed on the computer screen between stimulus presentations. The auditory stimulus was a 1 kHz FM tone (65 dB) presented through headphones. All stimuli were presented for 500 ms. On non-paired training trials and on trials presented during the scans, the interstimulus interval (ISI) ranged from 2 to 12 s (in 2 s increments, mean 7 s). On paired training trials, the visual stimulus was presented 250 ms after the onset of the auditory stimulus (Fig. 1*c*). Stimulus presentation and recording of responses was done using Superlab software (Cedrus) on a Macintosh LC II computer. A white curtain surrounded the visual field of the subject while in the scanner, and background illumination was dim to reduce the possibility of extraneous visual stimulation.

Task

The behavioral protocol is presented graphically in Figure 1*b*. Subjects were told that three stimuli would be presented, two visual and one auditory. The thick-lined circle was designated as the target and the other the distractor, and subjects pressed a key on a keyboard using their right hand when it appeared. The temporal relation between the auditory stimulus and the two visual stimuli was manipulated in two phases (low probability and high probability). During the low-probability phase, 12% of tones predicted a visual event [P(visual stimulus|tone) = 0.12] and this was increased to 80% in the high-probability phase [P(visual stimulus|tone) = 0.80]. To ensure equivalent learning to the two visual stimuli, equal numbers of targets and distractors were presented and the tone preceded the target and distractor an equal number of times. The use of two probabilities allows for the examination of brain systems involved in basic perceptual processing, and how they change following the introduction of the temporal relation. We expected that following the change in the temporal relation, the predictive ability of the tone would increase, and reaction times on paired trials, where the tone preceded the target, would become faster than on unpaired target-alone trials. Reaction time measures (RT) have been used before as a reliable index of conditioned expectancy (Perruchet, 1985).

Scans

Each scan consisted of 10 presentations of the single stimulus, and are analogous to CS probe trials in a standard classical conditioning experiment. All six scans were embedded within a series of training trials to minimize awareness of the scan. The first two PET scans, one of the visual distractor and one of the tone, were taken during the low-probability phase. The four remaining scans, three tone scans followed by one visual distractor scan, were done during the high-probability phase.

The experiment began with 10 training trials before scan 1 and 11 training trials after. For the remaining scans there were 25 training trials before and 25 training trials after the scan, then a 2 min break (5 min between scans 1 and 2). The tone scan taken during the low-probability phase measured the activity elicited by the tone when it had little association with a visual event (tone − low probability: TLP). Scans 3–5 (tone − high probability: THP1–3) provided a measure of tone-elicited activity as the association between the tone and visual events was acquired. It should be noted that because the target visual stimulus was never presented during scans, motor responses were not made during the scans.

In addition to these learning-related changes in activity, this combination of scans allowed us to address two important non-associative factors. First, since acquisition of the association between auditory and visual stimuli proceeded forward in time, the changes of rCBF reflecting acquisition would be confounded with non-specific effects of time such as adaptation and sensitization. These non-specific effects were expected to be revealed as sequential changes across all six scans, regardless of stimulus modality. A second non-associatve factor in this task is the discrimination between auditory and visual modalities. The inclusion of scans consisting of only auditory or visual stimuli allowed us to determine explicitly those brain regions simply involved in differentiating the stimulus modality, independent of learning-related effects. As we expected to identify neural patterns related to these non-associative
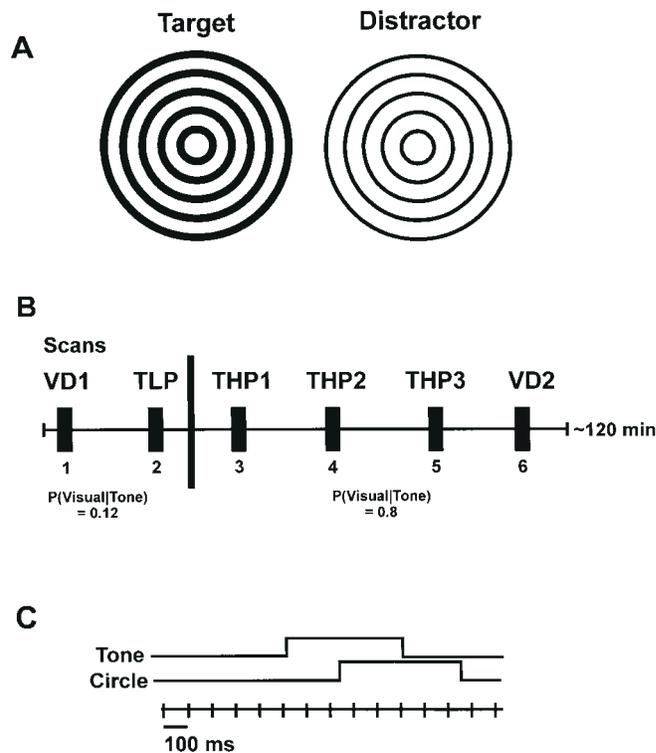

Figure 1. Schematic of experiment. (*A*) Representation of visual stimuli. Subjects were asked to press a button whenever the visual target was present. (*B*) Time line of experiment. First and second PET scans (visual distractor, VD1 and tone-low probability, TLP) were conducted following a block of trials when the tone did not predict the visual stimuli. The thick vertical line after the TLP scan marks the change in tone significance such that, across trials, the probability that a visual stimulus would follow the tone increased to 80% (THP). Scans 3–5 were of the tone alone (THP1–3) and the final scan was of the visual distractor (VD2). (*C*) Time line indicating the 250 ms overlap of the tone and visual stimulus on a trial in which the tone predicted a visual event.

factors, they were explicitly modeled in the statistical analysis (see below).

After the experiment concluded, subjects were debriefed to ascertain whether they had any overt awareness of the stimulus relations and then they were informed as to the relation among stimuli.

Image Analysis

All images from a subjects were spatially transformed to facilitate intersubject averaging and identification of common areas of change. For a subject, all image volumes were registered to the initial scan to correct for head motion across the experiment (AIR software, Woods *et al.*, 1992). The images were then transformed to an rCBF template conforming to a standard brain atlas space (Talairach and Tournoux, 1988), and smoothed with a 10 mm isotropic Gaussian filter to reduce individual anatomic variability (SPM95, Friston *et al.*, 1996). Voxel values within a transformed image volume were then expressed as a ratio of the average counts for all brain voxels within a scan.

Partial Least Squares

PLS was chosen as the primary analytic tool because it is optimized to detect activity patterns across the entire brain. In this study we examined these activity patterns as they related to two fundamental aspects of learning: stimulus parameters and behavioral outcome. Three separate PLS analyses were applied to these data to answer the three questions we had posed. The first analysis, design–brain PLS, examined the relations between experimental design factors and brain activity. The design–brain PLS was conducted to reveal how the change in the associative significance of the tone was expressed in the brain. The second analysis, brain–behavior PLS, examined the relations between behavior immediately preceding each scan with rCBF within the scan. This

brain–behavior PLS identified the neural systems showing a change in the relation to behavior as the association was learned. The final analysis, design–brain–behavior PLS, revealed the overlap between the system involved in processing the change in the significance of the auditory stimulus and that which mediated the change in behavior. The final analysis has been implemented in other contexts (Streissguth *et al.*, 1995) and here we use it to address a neurophysiological question.

Implementation and Interpretation of PLS

PLS is a family of multivariate statistical techniques that describes the relations between any set of exogenous measures, like experimental design or behavioral measures, and a set of dependent measures, in the present case brain images. PLS has been used extensively for one-dimensional images from spectrographs, as in chemometrics or remote sensing, and in toxicology and behavioral teratology (e.g. Hellberg *et al.*, 1986; Heise *et al.*, 1989; Streissguth *et al.*, 1993), and more recently has been adapted for use with functional imaging data (McIntosh *et al.*, 1996a; Nyberg *et al.*, 1996a; Schreurs *et al.*, 1997). The term 'partial least squares' refers to the computation of the optimal least-squares fit to part of a correlation matrix. This part is the 'cross-block' correlation between the exogenous and dependent measures. PLS is similar to principal components or eigenimage analysis (Moeller *et al.*, 1987; Friston *et al.*, 1993), but one important feature of PLS is that we constrain the solutions by incorporating prior knowledge of experimental design (scans) or behavior. Moreover, it is ideal for data sets where the measure within a block are highly correlated (e.g. the brain) because items within a block are not adjusted for these correlations (cf. canonical correlation).

We present the essential details of the three PLS analyses here; a more explicit mathematical description of PLS can be found in McIntosh *et al.* (1996a). For the design–brain PLS, the cross-block correlation between orthonormal design contrasts and each voxel of the image data set were examined. Two of these contrasts explicitly coded the two non-associative effects: time effects and stimulus modality. For the brain–behavior PLS, scan-specific correlations were computed between the rCBF within a scan and the behavior measure preceding that scan. These correlation 'maps' made up the cross-block correlation matrix. Singular value decomposition (SVD) was used to decompose the cross-block correlation matrix into orthogonal pairs of singular vectors or latent variables (LVs), which account for the covariance in the matrix in decreasing order of importance. These vector pairs reflect a symmetric relationship between those components of the experimental design (or behavior) most related to brain activity on one hand, and the optimal pattern of image-wide activity related to the identified design/behavior components on the other. This second vector can be displayed in image space, and because it is derived from SVD, we have called it a singular image; the numerical weights within the image are called saliences. The singular image from the design–brain PLS identifies the collection of voxels that as a group is most related to the design effects expressed in the LV. The singular image from the behavior-brain PLS identifies the collection of voxels that as a group relate to a change in behavior.

A second piece of information obtained from PLS are brain scores for each latent variable, which are similar to factor scores. Brain scores indicate how strongly individual subjects express the patterns on the latent variable. The scores are the dot product of subject's within-scan rCBF and the singular image on a particular LV. In the design–brain PLS, we plot brain scores by scan to show the subject variation in the singular image across scans. In the brain–behavior PLS, we plot behavior by brain scores within each scan to indicate those points in the experiment when brain–behavior correlations are similar and when they differ.

Assessment of Significance

Statistical assesment for PLS was done using permutation tests and bootstrap estimation of standard errors. The permutation test assessed whether the effect represented in a given singular image is sufficiently strong, in a statistical sense, and the standard error estimates of saliences assessed the reliability of peak saliences in the singular image.

Statistical significance of each LV was assessed by computing the squared multiple correlation (R^2) from the regression of brain scores on the design contrasts for the design–brain PLS, and for the regression of brain scores on behavior for the brain–behavior PLS. Significance of the R^2 was assessed by means of a permutation test, using 2000 permutations (Edgington, 1980; McIntosh *et al.*, 1996a ; Braun *et al.*, 1998). Since the brain scores are derived in a single analytical step, it is not necessary to correct for multiple comparisons as is done for univariate image analyses (e.g. Worsley *et al.*, 1992; Friston *et al.*, 1995).

To determine the stability of the maximal saliences identified on the LVs, the standard errors of the saliences were estimated through 100 bootstrap samples (Efron and Tibshirani, 1986; Braun *et al.*, 1998). A salience whose value depends greatly on which subjects are in the sample is less precise than one that remains stable regardless of the sample is chosen (Sampson *et al.*, 1989). Figures and tables that present the results show regional maxima and minima where the salience was greater than twice the standard error. (The MATLAB and C-code for PLS is available through anonymous FTP at ftp.rotman-baycrest.on.ca/pub/randy/pls.)

To aid in the interpretation of the singular images, univariate analyses were performed for the peak voxels identified in the PLS analyses. Differences in activity across scans were assessed using a univariate repeated-measures regression analysis (Pedhazur, 1982; Grafton *et al.*, 1991) with three orthogonal contrasts. The first two contrasts coded the non-associative effects of time and modality effects (auditory versus visual). The third contrast compared the unpaired tone scan with paired tone scans. Correlations of behavior and rCBF within each scan were computed for voxels identified in the behavior–brain PLS. These regression and behavior correlations were used only as descriptive statistics. Inferences were based on the permutation and bootstrap tests described above.

Design–Brain–Behavior PLS

The two block cases examining design–brain or brain–behavior relations are simple implementations of PLS analysis. It can be extended to describe the relations among several blocks connected according to any path diagram (e.g. Streissguth *et al.*, 1993). The algorithm for the design–brain–behavior, or multiblock, PLS analysis is described in the appendix. The model tested here assumed the relation between design factors and behavior was mediated through the brain (i.e. no direct connection between design and behavior). This analysis operated simultaneously on the matrix of correlations between design contrasts and brain images and the matrix of correlations between brain images and behavior. Thus, the design–brain–behavior PLS identified the collection of voxels that showed a change in activity reflecting some component of the experimental manipulation and also showed a systematic relation to behavior.

Results

Behavior

Figure 2 shows the changes in mean RT to the target stimulus for unpaired and paired trials across scans 2–6. Behavior prior to scan 1 was not analyzed because of the small number of trials for this block. To facilitate the visualization of the learning curve, the reciprocal of RT has been plotted. A differential response on paired and unpaired trials emerged across the five blocks as assessed by repeated-measures ANOVA [scan × stimulus interaction: $F(4,36) = 4.69$, $P < 0.025$] and Newman–Keuls *post-hoc* analysis. RTs did not differ in the low-probability trials (TLP). When the predictability of the tone increased, we found an expected decrease in RT on paired trials (Hershenson, 1962), which was maintained throughout training (THP1, THP2, THP3, VD2 > TLP, $P < 0.01$). However, the facilitation of RT initially extended to both paired and unpaired trials, indicative of a generalized enhancement of RT (THP1, THP2> TLP, $P < 0.05$). By the end of training, RT on unpaired trials returned to baseline (TLP) levels (THP1 > THP3,VD2, $P < 0.05$). The finding of an initial generalization followed by the return to baseline on unpaired trials suggests that an associative process mediated the differential effects on RT. The pattern of change in RT seen in the present study has been observed in other behavioral
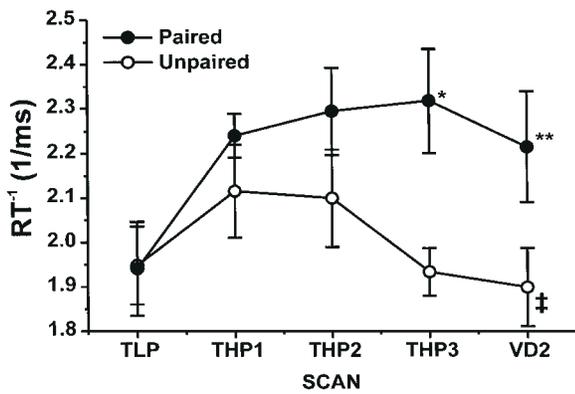
Figure 2. Mean reciprocal reaction time (1/s, ± standard errors) to the target visual stimulus for paired and unpaired trials preceding each of the last five PET scans; higher values indicate faster RTs. Significant differences between paired and unpaired trials are seen for THP3 and VD2 scans (Newman–Keuls, *$P < 0.05$, **$P < 0.01$). Significant slowing of RT on unpaired trials is also indicated (‡, VD2 < THP1,THP2, $P < 0.05$). Scan abbreviations are as in Figure 1.

conditioning studies (e.g. Perruchet, 1985). Based on debriefing reports, four subjects were aware of the temporal correlation between the auditory and visual stimuli. Those who detected the relationship did not differ behaviorally from those who did not.

Image Analysis

Design–Brain PLS

Five orthonormal (uncorrelated) contrasts were used for the design–brain PLS analysis. Two contrasts accounted for the non-associative factors: one represented a linear trend coding non-specific time effects, and the second compared the average of the two visual stimulus scans to the average of all tone scans to identify general modality differences. The remaining three contrasts compared each tone scan to the average of subsequent ones (i.e. TLP versus the mean of THP1, THP2, and THP3, etc.; these are also known as Helmert contrasts). It is important to note that the outcome of the design–brain PLS is the same if the two non-associative factors are removed prior to the analysis of experimental effects.

Five latent variables were identified, and the first two accounted for the expected non-specific time effect and the differences between auditory and visual stimulation respectively. Plots of brain scores by scan for LV1 and 2 are shown in Figure 3. The plot for LV1 (Fig. 3*A*) shows a progressive decrease in brain scores across time, which indicates a general time effect. This is probably a combination of adaptation or sensitization and perhaps motor learning as subjects became more proficient at responding to the target. The first singular image (not shown) identified ventral occipital and occipitotemporal regions showing positive saliences (positively correlated with the pattern of scores, i.e. decreases in rCBF across scans), while negative saliences clustered around motor, premotor and anterior cingulate cortices (increases in rCBF across scans). The pattern of scores on LV2 (Fig. 3*B*) distinguished between visual and auditory modalities, with the largest difference between the two visual scans (VD1 and VD2) and the first two tone-only scans (TLP and THP1). The lower scores for scans THP2 and THP3 may reflect habituation to the tone, although the significance of the difference in these brain scores compared to TLP and THP1 was not formally tested. The singular image identified bilateral superior temporal regions of positive salience (greater rCBF
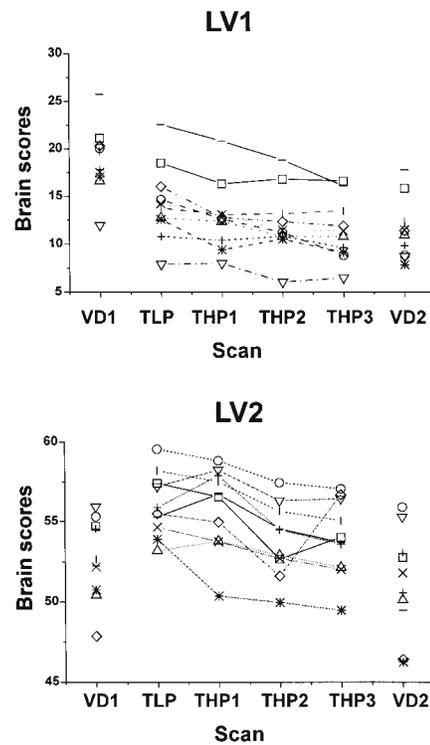

Figure 3. Scatterplots of brain scores by scan for the first (LV1) and second (LV2) latent variables for the design–brain partial least squares analysis. Each subject is indicated by a different symbol, and brain scores are connected by a line across tone scans. Scan abbreviations are as in Figure 1.

Table 1
Local maxima and minima in the third singular image for partial least squares analysis of design

Bootstrap ratio	F	Fprob	x	y	z	Gyrus and area
Maxima						
2.09	4.99	*0.03*	24	−16	−4	putamen
2.57	7.55	*0.008*	40	−50	−4	fusiform – 37
2.39	4.90	*0.03*	−10	−90	4	cuneus – 17/18
2.60	7.43	*0.009*	46	4	32	precentral – 6
2.06	6.52	*0.01*	40	−2	44	precentral – 4
2.55	7.06	*0.01*	28	−40	40	inferior parietal – 40
Minima						
−2.47	17.49	*0.0001*	10	4	−12	subcallosal 25
−2.62	6.26	*0.016*	−4	42	8	cingulate – 32
−2.61	4.62	*0.04*	−6	48	8	dorsomedial frontal – 10
−2.35	6.93	*0.01*	−16	40	20	dorsomedial frontal – 8
−2.70	10.35	*0.002*	20	42	28	superior frontal – 9
−2.52	6.38	*0.015*	−18	34	44	superior frontal – 8

Locations are given in stereotaxic coordinates, approximate Brodmann area and gyral location. Bootstrap ratios are the salience for a given maximum or minimum divided by its bootstrap estimated standard error. Univariate F and probability (Fprob) are from a univariate regression analysis.

during tone scans) and primary visual cortices showing negative saliences (greater rCBF during visual distractor scans). Both LV1 and LV2 were statistically significant according to permutation tests (LV1: $R^2 = 0.36$, $P \approx 0.014$; LV2: $R^2 = 0.33$, $P \approx 0.015$).

The activity pattern most congruent with the change in significance of the tone was observed on LV3. The singular image and scores for this LV are presented in Figure 4, and this LV was statistically significant ($R^2 = 0.34$, $P \approx 0.015$). The maxima from the singular image, univariate summary statistics and stereotaxic coordinates are shown in Table 1. The pattern of
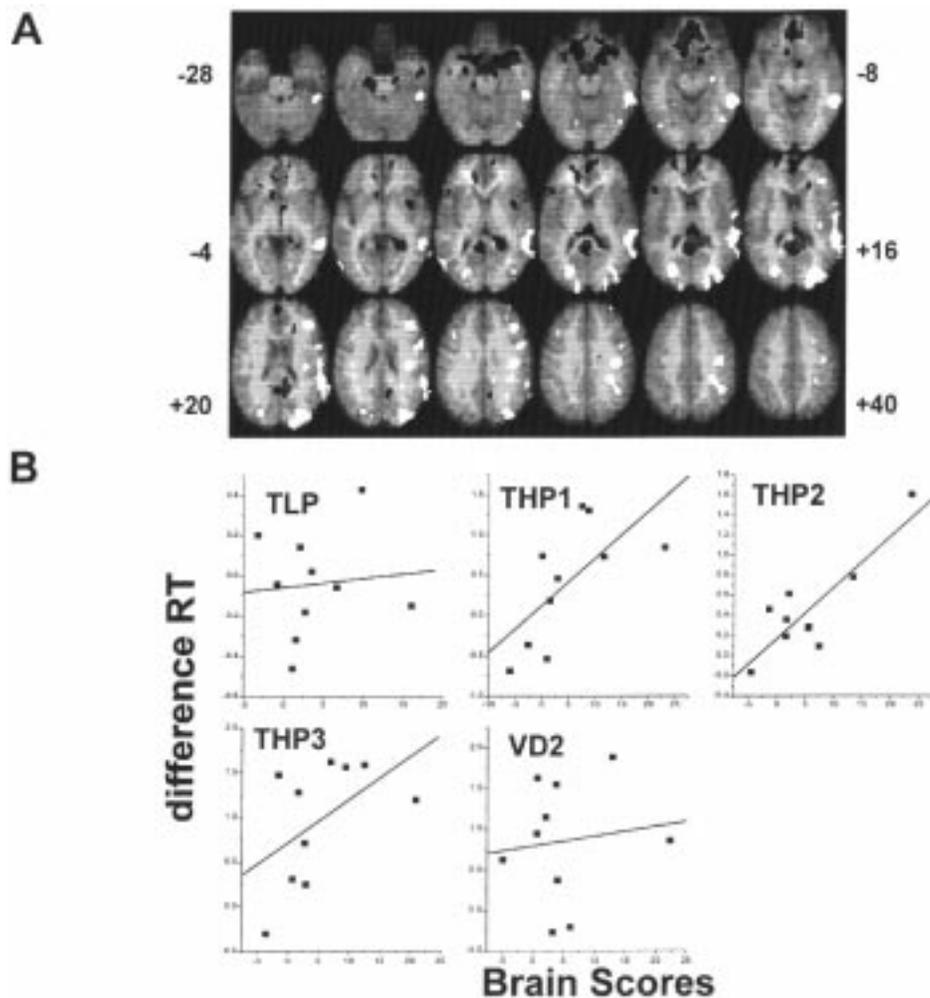
Figure 4. Third latent variable from the design–brain partial least squares analysis. The singular image (*A*) is overlaid on horizontal sections from a structural MRI that conforms to the atlas space of Talairach and Tourneaux (1988). Slices start at −28 mm from the anterior commissure–posterior commissure line at the top left slice and move in increments of 4 mm to +40 mm at the bottom right; left is the subject's left and the top is anterior in the image. Voxels with saliences greater than twice their standard error are shown, with positive saliences in white and negative in black. (*B*) Plot of the brain scores for each subject across scans; each subject is indicated by a different symbol with brain scores connected by a line across tone scans. Scan abbreviations are as in Figure 1.

brain scores from scan 2 (TLP) through to scan 5 (THP3) very much resembles an acquisition curve (Fig. 5*B*). Maximum positive saliences for LV3 included right inferior temporal and fusiform gyrus [Brodmann area (BA) 37], a large area starting in the right midbrain with a peak in the ventral–caudal putamen, left cuneus cortex (BA 17 and 18); right lateral extrastriate was salient but somewhat less reliable than the left occipital area. Right inferior parietal (BA 40), premotor (BA 6) and precentral (BA 4) cortices were also reliably salient on this LV. Peak negative saliences were observed in a large expanse of medial prefrontal cortex starting from a ventral region near the ventral extent of the anterior cingulate to a more dorsal component anterior to the genu of the corpus callosum, which extended rostrally to include BA 10 and the medial expanse of BA 8. Right dorsolateral prefrontal cortex was also negatively salient (BA 9). The pattern of brain scores across the scan conditions suggests this LV represents, first, the detection of the change in the temporal correlation from low to high probability. This is indicated by the

striking separation of the TLP scan from the other tone scans (Fig. 4*B*). Secondly, this LV represents the change in associative strength of the tone as the auditory visual association was learned. With reference to the experimental question, the singular image for LV3 represents the pattern of image-wide activity most related to processing the change in the associative value of the tone.

The final two LVs were not significant by permutation tests and the maximum saliences had unacceptably large variances by bootstrap, which corresponded to a weaker spatial signal than seen on the preceding three LVs. These LVs were not considered further.

Brain–Behavior PLS

The index of associative learning used for this analysis was the difference in mean reaction time (diffRT) between paired and unpaired trials for a subject across all training trials preceding scans 2–6. As for the analysis of mean RT, the first scan was not

Figure 5. First latent variable from the brain–behavior partial least squares analysis. The singular image (*A*) is overlaid on horizontal sections from a structural MRI as in Figure 4. The scatterplots (*B*) are the difference in reaction time between paired and unpaired trials by brain scores within each of the five scans used in the analysis. The scatterplots show the strong relation of difference RT and brain scores for the THP scans, but relatively weaker relation in the TLP and final visual distractor scan (VD2).

included since there was not a sufficient number of trials with RT measures. For each of the five scans, the correlation of diffRT and each voxel was computed, resulting a brain–behavior correlation map for that scan. The PLS analysis was done on these five correlation maps.

Five latent variable pairs were also identified on this analysis. Of these, the first was most related to the change in the behavior, and was significant by permutation test ($R^2 = 0.52$, $P \approx 0.008$). Of particular interest on this LV was the change in the covariation pattern across the four tone scans, which can be seen in the scatterplots of the behavior with brain scores within each scan (Fig. 5*B*) where larger values for behavior indicate faster RTs on paired than unpaired trials and thus better learning. There was no correlation between behavior and brain scores for the TLP scan, which switched to strong positive correlations for the three THP scans. The correlation on the final scan, which reflected the relation between diffRT and the activity elicited by the visual distractor in salient areas, was low and similar to that seen for the TLP scan. We expected the neural representation of the change in behavior to reflect the significance of the tone, and this is shown in three aspects of this LV. First, the tone did not have associative significance preceding the TLP scan (pre-TLP, Fig. 2), and activity elicited by the tone on this scan

was not correlated with performance. Secondly, as learning proceeded (pre-THP1, THP2 and THP3), the correlations of behavior with activity elicited by the tone were strong. Finally, the correlations were specific to the tone, which can be seen in the lack of a relationship between the large diffRT at the end of training (pre-VD2, Fig. 2) and the activity elicited by the visual distractor. Because a marked change in the relation between brain and behavior scores occurred at the point in training when the differentiation between paired and unpaired trials emerged, we interpret this LV to represent the activity patterns supporting the behavioral response to the tone as the association between stimuli strengthened.

The neural system related to behavior is shown in the singular image for LV1 (Fig. 5*A*) and Table 2 lists maxima, univariate summary statistics, and their stereotaxic coordinates. The univariate correlations show that on the whole, the peak voxels identified on the LV showed a pattern of correlations distinguishing the three THP scans from the TLP and VD2 scans. For areas with negative saliences, increased rCBF was associated with smaller diffRTs, and conversely, for areas with positive saliences, increased rCBF was associated with larger diffRTs. Regions showing negative saliences included a similar expanse of medial prefrontal cortex to that noted for the design analysis.

Table 2

Local maxima and minima in the first singular image for partial least squares analysis of behavior

Bootstrap ratio	r(TLP)	r(THP1)	r(THP2)	r(THP3)	r(VD2)	x	y	z	Gyrus and area
Maxima									
3.21	0.44	0.81	0.57	0.71	0.03	36	−20	28	postcentral − 3
3.14	−0.28	0.53	0.79	0.38	0.05	50	−16	20	postcentral − 1 and 2
2.90	−0.14	0.26	0.58	0.72	0.15	40	0	28	precentral − 6
3.29	−0.07	0.77	0.80	0.26	−0.22	44	−48	−8	inferior temporal − 37
2.78	0.39	0.45	0.53	0.21	0.09	−12	−90	12	superior occipital/cuneus − 18
3.26	0.46	0.45	0.35	0.21	−0.34	−4	−84	16	superior occipital − 18/19
3.19	0.23	0.74	0.62	0.18	−0.11	28	−78	24	superior occipital
3.37	−0.18	0.45	0.50	0.25	−0.54	16	−94	28	cuneus − 18
3.12	−0.05	0.43	0.60	0.75	−0.32	−28	−80	16	medial occipital − 19
2.86	−0.15	0.63	−0.26	0.19	0.13	−56	6	16	inferior frontal − 44
3.44	−0.42	0.35	0.27	0.18	−0.42	−52	−10	28	postcentral − 1 and 2
3.09	0.29	0.49	0.51	0.63	0.04	30	30	24	middle frontal − 46
2.77	0.15	0.65	0.58	0.68	0.10	28	−38	32	inferior parietal − 40
Minima									
−3.07	0.60	−0.83	−0.39	−0.41	0.43	10	4	−12	subcallosal − 25
−3.29	0.04	−0.77	−0.34	−0.55	0.24	32	14	−16	inferior frontal − 47
−3.04	0.24	−0.40	−0.83	−0.56	0.22	−6	34	−12	cingulate − 32
−3.23	−0.13	−0.43	−0.77	−0.25	0.37	10	56	0	superior frontal − 10/11
−3.22	−0.27	−0.77	−0.21	−0.57	−0.07	8	−38	8	retrosplenial − 30
−3.16	0.08	−0.46	−0.52	−0.43	−0.27	−22	58	12	dorsomedial frontal − 9 / 10

Locations are given in stereotaxic coordinates, approximate Brodmann area and gyral location. Bootstrap ratios are the salience for a given maximum or minimum divided by its bootstrap estimated standard error. Columns r are the correlation of RT difference and rCBF at the voxel for each of the five scan conditions (TLP = tone, low-probability phase; THP1–3 = tone scans 1–3, during high-probability phase, VD2 = visual distractor scan 2). A correlation of 0.64 has a probability of 0.05.

More dorsally, a region of negative saliences was noted in the right hemisphere, which spanned the retrosplenial cortex (BA 29/30). Areas with positive saliences were mainly in right hemisphere with the exception of dorsal and lateral occipital cortices (BA 18/19). Opposite to the pattern in the design–brain analysis, the salient right occipital areas were extensive than the left. A large expanse of positive saliences were also present in right inferior to middle temporal cortex (BA 37), right and left premotor cortices and right prefrontal areas (BA 6 and 46 respectively).

Design–Brain–Behavior PLS

This analysis revealed brain areas common to both the design and behavior for scans 2-6. Three matrices were used: a matrix of four orthonormal Helmert contrasts, the diffRT measures (from the brain-behavior PLS), and the corresponding brain images from the five scans. One singular image was identified and its pattern of scores shows the strongest convergence of the effects of design and behavior. Specifically, this reflected the change in associative significance of the tone. The patterns of scores and saliences were opposite in sign, but otherwise similar to those seen for LV3 in the design-brain PLS and LV1 in the brain–behavior PLS, both of which revealed learning-related changes.

The singular image representing those brain regions simultaneously related to design effects and behavior is presented in Figure 6. The dominant areas on the singular image with positive saliences were the ventral anterior cingulate, medial prefrontal cortex and right posterior cingulate extending into retrosplenial cortex. Negative saliences were prominent in the right hemisphere in the middle and superior temporal gyrus, near auditory association cortices, bilateral occipital cortices, anterior parietal, premotor, and somatosensory and bilateral motor cortices. Table 3 presents the stereotaxic coordinates, minima and maxima from the singular image, and univariate summary statistics.

The pattern of scores for the design side of the model was similar to that seen on LV3 in the design–brain PLS, and distinguished the TLP scan from THP2 and THP3. The singular images from these two LVs had a correlation of -0.53, indicating a moderate overlap. The correlations of the design–brain-behavior singular image with those from LV1 and LV2 in the design–brain PLS were much lower (0.12 and 0.09 respectively), indicating that the collection of regions represented on LV1 and 2 was not contributing to the observed pattern from the design-brain–behavior analysis.

The correlation of brain scores to diffRT in the design-brain-behavior analysis was very similar to LV1 in the brain–behavior analysis (correlation between singular images = −0.88). As in the brain-behavior analysis, strong relations between brain scores and diffRT were seen only on the THP scans.

To estimate the strength of the influences in the putative causal model linking design, brain and behavior, the correlations between the design contrasts and brain scores, and brain scores and behavior were calculated. The relation of the design and brain scores was substantially weaker ($r = 0.15$) than the corresponding one between brain and behavior ($r = 0.53$). This suggests that the salient areas showed variations in activity across the tone scans, but were primarily related to behavior. This difference in correlations is born out by inspection of the scatterplots in the bottom of Figure 6, where the scatter is much more variable in relation to design (Fig. 6B), than in relation to behavior (Fig. 6C). That the salient regions identified in the final PLS analysis were more associated with behavior is also evident from examination of the univariate statistics in Table 3. More areas showed moderate to high correlations with diffRT in the THP scans than areas showing significant variation in mean rCBF across scans.

Bilateral superior prefrontal cortex (BA 8 and 9) identified in the design-brain analysis was not salient in the present analysis (Fig. 6) or in the brain-behavior analysis (Fig. 5). In fact, the salience estimates for these regions on the singular image related to behavior were very near zero, suggesting that while these
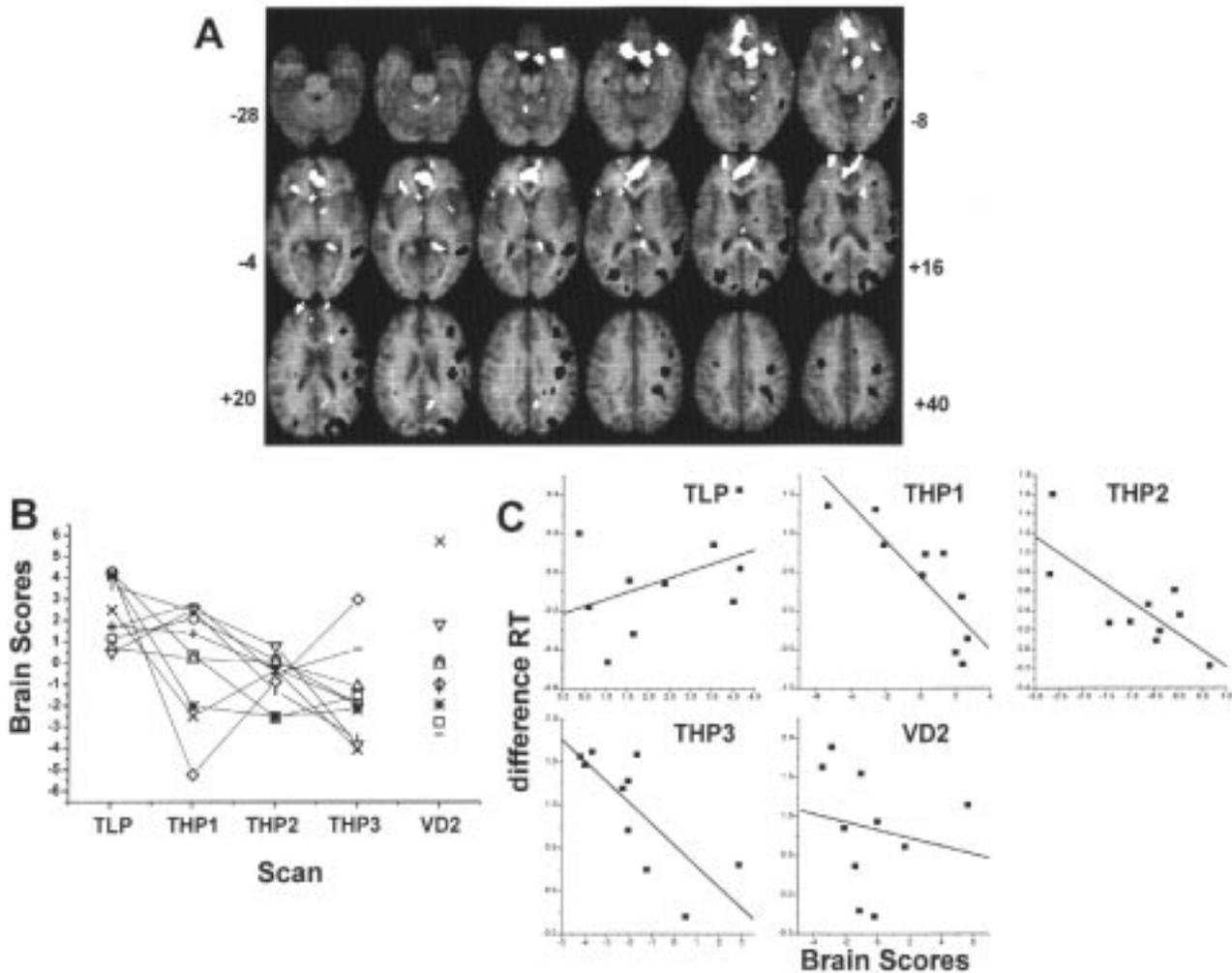
Figure 6. Results from the design–brain–behavior partial least squares analysis. The singular image (*A*) is overlaid on horizontal sections from a structural MRI as in Figure 4. Saliences in the image were thresholded at an arbitrary value of 0.3 (absolute). The singular image is effectively a mirror image amalgamation of those presented in Figures 4 and 5. Areas negatively salient (colored black) showed greater rCBF in THP scans compared to TLP, while positively salient areas (colored white) showed greater rCBF in the TLP scan. In terms of difference RT, regions of negative saliences showed positive correlations with difference RT in the THP scans and areas that were positively salient were negatively correlated with difference RT in the THP scans.

regions were involved in processing the significance of the stimuli (Fig. 5), they were not part of the neural system that showed a learning-related change in its effect on behavior (Fig. 6).

Discussion

Neuroscience investigations most often explore design and brain, or behavior and brain relations, two domains at a time. Here, we explore the three domains together, and find that there is overlap between the pattern of activity related to the changed associative value of the tone and the pattern related to behavioral change. Such an alignment argues for a central role of the identified functional system in processing the change in stimulus contingencies and in utilizing this information in an associative manner to coordinate the behavioral response in this task. The brain areas in this pattern were less related to the stimulus, or design, than to the response. In the present study, this is not surprising: the physical parameters of the stimuli did not change, only their meaning. But in studies where the stimulus parameters or cognitive processes differ between tasks, a stronger relation of the design to brain activity may be expected.

Changes in activation patterns in response to the tone were identified when there was no change in visual stimulation and no motor response. The patterns of activity measured during the scans arose in response to non-target stimuli. In tone scans, only the tone was presented; during the distractor scans, only the visual distractor was presented. Design–brain PLS LV3 identified a pattern of activity that differentiated low- from high-probability tones. Since activity patterns that could be attributed to non-specific time effects and differences in stimulus modality were accounted for on other, independent, singular images (LV1 and 2), the pattern across the LV3 singular image elicited by the tone most likely reflects the emergence of a learned expectancy of the tone–visual stimulus relationship.

The brain–behavior PLS identified a strong pattern of image-wide covariance that we interpret as reflecting a neural system subserving the conditioned use of the auditory–visual stimulus relation to affect performance. Using behavioral data acquired up to the point of scanning, we noted a systematic and robust relation of brain and behavior that preceded the change in the behavioral response. The RTs for paired and unpaired trials were not significantly different for the THP1 scan, but the correlation

Table 3
Local maxima and minima in the singular image for design–brain–behavior partial least squares analysis

Salience	F	Fprob	r(TLP)	r(TH12)	r(THP2)	r(THP3)	r(VD2)	x	y	z	Gyrus and area
Maxima											
0.52	17.49	0.0001	0.60	–0.83	–0.39	–0.40	0.43	10	4	–12	subcallosal – 25
0.40	9.46	0.0035	0.12	–0.67	–0.61	–0.12	0.22	4	48	12	dorsomedial frontal – 10
0.39	6.36	0.02	0.13	–0.63	–0.42	–0.43	0.27	–4	44	8	cingulate – 32
0.47	3.04	0.08	0.04	–0.77	–0.34	–0.55	0.24	32	14	–16	inferior frontal – 47
0.38	0.02	0.96	–0.27	–0.77	–0.21	–0.57	–0.07	8	–38	8	retrosplenial – 30
0.43	2.04	0.16	0.24	–0.66	–0.14	–0.77	0.55	–26	28	0	inferior frontal – 47/11
0.40	2.42	0.13	–0.15	–0.69	–0.31	–0.47	–0.44	–20	64	16	dorsomedial frontal – 10
Minima											
–0.47	0.18	0.67	–0.27	0.52	0.79	0.37	0.04	50	–16	20	postcentral – 1 and 2
–0.44	7.38	0.01	0.11	0.46	0.64	0.64	0.47	50	–40	12	superior temporal – 22
–0.43	6.09	0.02	–0.23	0.75	0.67	0.14	–0.41	44	–50	–8	inferior temporal – 37
–0.41	2.37	0.13	0.21	0.62	0.31	0.42	0.32	26	–16	–8	putamen/midbrain
–0.41	2.53	0.12	–0.05	0.43	0.60	0.75	–0.32	–28	–80	16	medial occipital – 19
–0.44	2.70	0.11	0.23	0.74	0.62	0.18	–0.11	28	–78	24	superior occipital – 19
–0.36	0.14	0.71	0.15	0.54	0.53	0.37	0.05	14	–90	20	cuneus – 18
–0.38	0.26	0.61	0.04	0.72	–0.19	0.12	0.35	–58	6	12	inferior frontal – 44
–0.31	1.15	0.28	–0.06	0.43	0.22	0.16	0.38	–54	0	32	precentral – 6
–0.55	1.88	0.17	0.44	0.81	0.57	0.71	0.02	36	–20	28	postcentral – 3
–0.47	10.76	0.002	–0.17	0.28	0.72	0.76	0.24	42	2	28	precentral – 4
–0.42	0.52	0.47	0.29	0.49	0.51	0.63	0.04	30	30	24	middle frontal – 46
–0.46	3.99	0.06	0.15	0.65	0.58	0.67	0.10	28	–38	32	inferior parietal – 40

Locations are given in stereotaxic coordinates, approximate Brodmann area and gyral location. Saliences are the weights for the voxel, indicating the strength of the relation to the combined latent variable for design and behavior. Univariate F and r are the same as in the preceding tables.

between brain scores and behavior was strong and was maintained across subsequent THP scans. This indicates that the system processing the associative significance of the tone was related to performance early in training, before the complete separation between paired and unpaired RT emerged for all subjects (see Fig. 2). This neural system responded uniquely to the tone, since activity elicited by the visual distractor in this collection of regions did not relate to behavior, even though the difference between paired and unpaired trials was still large by this point in the experiment. Since the singular image was reliable across subjects (as indicated by bootstrap), the interpretation of the neural system as that most related to the associative response to the tone that affected behavioral change is warranted.

At a general level, the singular images from all the three PLS analyses identified a common distributed neural system consisting of a more lateral 'sensory-motor' component and a more medial 'frontal-limbic' part. The sensory-motor component consisted of pre- and postcentral cortical regions, temporal cortices near auditory associated regions, and occipital cortices. The frontal-limbic system consisted mainly of medial prefrontal areas including anterior cingulate and posterior regions around retrosplenial cortex. Regions in the lateral sensory-motor component (positively salient in Figs 4 and 5, and negatively salient in Fig. 6) showed greater activity as the tone acquired associative meaning and were positively correlated with performance. The frontal-limbic component (areas negatively salient in Figs 4 and 5, and positively salient in Fig. 6) showed decreasing activity as the tone acquired associative meaning and was negatively correlated with performance. These two components were most evident in the design–brain–behavior PLS analysis (Table 3).

The PLS analysis uses information from throughout the image. The contributions of areas across a singular image are not equal, in the sense that there is variation in the saliences across regions, but the areas are identified because they respond as a system to the design manipulations, and act as a system to affect behavior.

The brain scores derived from PLS act as the index of this system-level activity. Examination of the saliences across singular images (with constraints based on the reliability of the salience estimate) provides an assessment of the regional contribution to the activity of the distributed system. The constituents of the system identified in the present study correspond well to those identified in other studies of associative or procedural learning tasks, as we elaborate below.

Regional Contributions
Of the areas that were salient on the singular images, the dorsal prefrontal regions (BA 8 and 9) were found only in the design–brain analysis and were part of the medial prefrontal-limbic component. These cortical areas have been identified in other PET studies of motor learning (Grafton *et al.*, 1995; Jueptner *et al.*, 1997), eyeblink conditioning (Schreurs *et al.*, 1997) and conditional associative learning (Petrides *et al.*, 1993), suggesting they may have some role in associative behaviors. Lesion studies have shown that dorsal frontal damage compromises some associative behaviors (Petrides, 1985; Petrides and Pandya, 1994). Based on the present findings, the role of these prefrontal areas may be in task demands not related to the actual response. A possible interpretation is that these areas are allied with detection of the association between stimuli, but that the impact on behavior is propagated onto other areas.

Both temporal (perhaps auditory association) and occipital cortices showed changing activity patterns across the experiment that related to both task and to behavior. Several investigators have noted changes in sensory cortices as the behavioral relevance of sensory stimuli changed. Such learning-related effects have been detected in primary sensory structures as early as the cochlear nuclei in the auditory system (Woody *et al.*, 1992), and in primary auditory cortex in monkeys (Recanzone *et al.*, 1992) and humans (Molchan *et al.*, 1994; Schreurs *et al.*, 1997). Our results add to these by showing that learning about a stimulus in one sensory domain (auditory) can affect activity in areas in the domain of the associated stimulus

(visual). Perception in a natural environment frequently involves the combination of sensorial experiences (Stein and Meredith, 1993), and thus information from one sensory modality will influence perception in another. Psychophysical studies have shown cross-modal influences between auditory and visual systems in the perception of motion, stimulus intensity and speech (McGurk and Macdonald, 1976; Stein *et al.*, 1996; Sekuler and Sekuler, 1997). Early evoked potential (EP) work (Durup and Fessard, 1935) noted that an EP at the occipital electrodes developed as an auditory stimulus came to predict a visual event. More recently, the reverse influence was observed in the rat, where activity in auditory cortex was elicited by the presentation of a light that predicted a tone (Cahill *et al.*, 1996). EP measures taken in humans during sensori-sensorial association of auditory with visual stimuli showed a focal increase in the auditory EP at electrodes located over the occipital lobe (Bruneau *et al.*, 1990). This is closely analogous to the results we obtained in the present study. What we add to the EP results is the possibility that the learning-related changes in occipital activity resulted from the acquisition of the auditory–visual associations. Moreover, the occipital regions are also part of the distributed neural system that is related to behavior. The distributed nature of stimulus–response mapping is confirmed by single-cell work in monkey motor cortex, where cell firing patterns show strong temporal covariance with the presentation of the signal stimulus and with the coordination and execution of the response (Zhang *et al.*, 1997). Similar patterns of cell responding have been observed in the hippocampus and adjacent cortical areas (Wilson *et al.*, 1990).

One possible factor that may have contributed to the changes in occipital cortex was focused attention to the visual domain in anticipation of an upcoming target. Event-related potential studies have found that shifts in visual attention modulate activity in extrastriate but not striate cortices (Clark and Hillyard, 1996). However, the occipital area identified presently was part of a larger system whose activity changed across scans as the association was acquired. Such a change would not be expected if attention was the only modulating effect. We favor the interpretation that the change of activity in the occipital areas resulted from a learned expectancy concerning the tone and visual stimuli. In this view, learning and attentional processes are not independent, but work together in identifying salient features in the environment and using that information to facilitate responses. Such a position has been echoed by some learning theorists who view associative learning as the reallocation of attention to what is important in the environment (Mackintosh, 1975).

Motor and somatosensory cortices were salient, but more so in the right hemisphere, ipsilateral to the hand making the response. Such laterality has been noted in some other PET motor learning studies (Seitz *et al.*, 1990; Grafton *et al.*, 1995); it is not clear why. Since there were no responses during the scans, the activity in sensorimotor regions may reflect anticipation of the response rather than the response *per se*. Studies that have examined activation in anticipation of motor movements have noted changes in motor-related regions, several of which overlap those identified in the present study. The overlapping regions include not only sensorimotor (BA 3, 1 and 2) and premotor (BA 6) regions, but also dorsal prefrontal areas 8 and 9, and middle prefrontal area 10 (Deiber *et al.*, 1996). Similar to occipital and temporal cortices, the change in involvement of these regions could reflect increased anticipation of the required motor response subsequent to the auditory cueing of a visual event.

The putamen was part of the sensory-motor component and was most salient in the design–brain PLS analysis. Electrophysiological and 2-deoxyglucose mapping work has documented activity patterns in the striatum and connected midbrain structures related to the learned significance of stimuli (e.g. substantia nigra) (Gonzalez-Lima and Scheich, 1986; Apicella *et al.*, 1992; Schultz *et al.*, 1993). Furthermore, the regions of monkey striatum containing neurons sensitive to presentation of a behavioral cue seem to be distinct from those related to the actual execution of a learned motor response (Aosaki *et al.*, 1995; Brown *et al.*, 1995; Apicella *et al.*, 1992, 1997). Our results suggest that a similar segregation exists in the humans; confirmation awaits further study.

The anterior and posterior cingulate cortices were salient and were part of the medial frontal-limbic dimension. The regions of anterior cingulate cortex were much more ventral than those most related to the execution of a motor program (Paus *et al.*, 1993), and the posterior extent lay in the retrosplenial area in the transition between the hippocampus and cingulate cortex. A similar activity pattern has been observed that distinguished the learning of a series of faces from recognition of the encoded faces (McIntosh *et al.*, 1996a). Other PET studies of associative learning have identified posterior cingulate cortex activation that follows the change in stimulus associations (Molchan *et al.*, 1994; Schreurs *et al.*, 1997). Electrophysiological studies of associative learning in the rabbit by Gabriel and colleagues (for review see Gabriel, 1993) consistently note changes in cell firing patterns in anterior and posterior cingulate cortices that follow the acquisition of learned behavior.

In summary, the present results are congruent with the idea that in the course of normal operations, learning is the result of distributed interactions among several brain regions (McIntosh and Gonzalez-Lima, 1994). We identified a system, characterized along a sensory-motor and medial frontal limbic dimension, that, as a whole, showed a change in activity as the tone acquired significance and was related to the learning-related change in behavior. The specific dynamic relations among elements of this system await further elucidation (e.g. McIntosh and Gonzalez-Lima, 1994). At present it is helpful to interpret the identified patterns of image-wide activity as a functional system mediating the learned association between auditory and visual events. Other research that explicitly examines neural interactions has quantified changing interrelations related to learning and memory (McIntosh *et al.*, 1996b; Nyberg *et al.*, 1996b). Here we show the overlap of systems that detect and respond to changes in the temporal relations among stimuli, and systems that use the learned association to mediate behavior. In a sense, we have identified a neural pattern that simultaneously represents 'cause', the detection of a change in temporal contingency, and 'effect', the resultant change in behavior.

References

Aizawa H, Inase M, Mushiake H, Shima K, Tanji J (1991) Reorganization of activity in the supplementary motor area associated with motor learning and functional recovery. Exp Brain Res 84:668–671.

Aosaki T, Kimura M, Graybiel, AM (1995) Temporal and spatial characteristics of tonically active neurons of the primate's striatum. J Neurophysiol 73:1234–1252.

Apicella P, Scarnati E, Ljungberg T, Schultz W (1992) Neuronal activity in monkey striatum related to the expectation of predictable environmental events. J Neurophysiol 68, 945–960.

Apicella P, Legallet E, Trouche E (1997) Responses of tonically discharging neurons in the monkey striatum to primary rewards delivered during different behavioral states. Exp Brain Res 116:456–66.

Bakin JS, Weinberger NM (1990) Classical conditioning induces CS-specific receptive field plasticity in the auditory cortex of the guinea pig. Brain Res 536:271–286.

Blaton TA, Zeffiro TA, Gabrieli JD E, Bookheimer SY, Carrillo MC, Theodore WH, Disterhoft J F. (1996) Functional mapping of human learning: a PET activation study of eyeblink conditioning. J Neurosci 16:4032–4040.

Bower GH, Hilgard ER (1981) Theories of learning. Englewood Cliffs, NJ: Prentice Hall.

Braun AR, Balkin TJ, Wesensten NJ, Gwadry F, Carson RE, Varga M, Baldwin P, Belenky G, Herscovitch P (1998) Dissociated pattern of activity in visual cortices and their projections during human rapid eye movement sleep. Science 279:91–95.

Brown VJ, Desimone R, Mishkin M (1995) Responses of cells in the tail of the caudate nucleus during visual discrimination learning. J. Neurophysiol 74:1083–1094.

Bruneau N, Roux S, Garreau B, Martineau J, Lelord G (1990) Cortical evoked potentials as indicators of auditory-visual cross-modal association in young adults. Pav J Biol Sci 25: 201–207.

Cabeza R, Grady CL, Nyberg L, McIntosh AR, Tulving E, Kapur S, Jennings JM, Houle S and Craik FIM (1997) Age-related differences in neural activity during memory encoding and retrieval: a positron emission tomography study. J Neurosci 17:391–400.

Cahill L, Ohl F, Scheich H (1996) Alteration of auditory cortex activity with a visual stimulus through conditioning: a 2-deoxyglucose analysis. Neurobiol Learn Mem 65:213–222.

Channon S, Daum I, Gray J (1993) Operant conditioning after temporal lobe lesions in man: conditional and simple discrimination learning. Cortex 29:316–324.

Clark VP, Hillyard SA (1996) Spatial selective attention affects early extrastriate but not striate components of the visual evoked response. J Cognit Neurosci 8:387–402.

Daum I, Channon S, Gray J (1992) Classical conditioning after temporal lobe lesions in man: sparing of simple discrimination and extinction. Behav Brain Res 52:159–65.

Deiber MP, Ibanez V, Sadato N, Hallett M (1996) Cerebral structures participating in motor preparation in humans: a positron emission tomography study. J Neurophysiol 75:233–247.

Domjan M, Burkhard B (1982) The principles of learning and behavior. California: Brooks/Cole.

Durup PG, Fessard A (1935) L'Electrenencephalogramme de l'homme: observations psycho-physiologiques relative a l'action des stimuli visuels et auditifs. Ann Psychol 36:1–32.

Edgington ES (1980) Randomization tests. New York: Marcel Dekker.

Efron B, Tibshirani R (1986) Bootstrap methods for standard errors, confidence intervals and other measures of statistical accuracy. Statist Sci 1:54–77.

Friston KJ, Frith CD, Liddle PF, Frackowiak RSJ (1993) Functional connectivity: the principal-component analysis of large (PET) data sets. J Cereb Blood Flow Metabol 13:5–14.

Friston KJ, Holmes AP, Worsley KJ, Poline J-P, Frith CD, Frackowiak RSJ (1995) Statistical parametric maps in functional imaging: a general linear approach. Hum Brain Mapp 2:189–210.

Friston KJ, Ashburner J, Frith CD, Pline J-B, Heather JD, Frackowiak RSJ (1996) Spatial registration and normalization of images. Hum Brain Mapp 2:165–189.

Gabriel M (1993) Discriminative avoidance learning: a model system. In: Neurobiology of cingulate cortex and limbic thalamus: a comprehensive handbook (Vogt B, Gabriel M, eds), pp. 478–523. Boston, MA: Birkhauser.

Gonzalez-Lima F (1992) Brain imaging of auditory learning functions in rats: studies with fluorodeoxyglucose autoradiography and cytochrome oxidase histochemistry. In: Advances in metabolic mapping techniques for brain imaging of behavioral and learning functions (Gonzalez-Lima F, Finkenstaedt T, Scheich H, eds), Vol. 68, pp. 39–109. Dordrecht: Kluwer.

Gonzalez-Lima F, Scheich H (1986) Classical conditioning of tone-signaled bradycardia modifies 2-deoxyglucose uptake patterns in cortex, thalamus, habenula, caudate–putamen and hippocampal formation. Brain Res 363:239–256.

Grafton ST, Woods RP, Mazziotta JC, Phelps ME (1991) Somatotopic mapping of the primary motor cortex in humans: activation studies with cerebral blood flow and positron emission tomography. J Neurophysiol 66:735–743.

Grafton ST, Mazziotta J C, Presty S, Friston KJ, Frackowiak RSJ, Phelps ME (1992) Functional anatomy of human procedural learning determined with regional cerebral blood flow and PET. J Neurosci 12:2542–2548.

Grafton ST, Hazeltine E, Ivry R (1995) Functional mapping of sequence learning in normal humans. J Cognit Neurosci 7:497–510.

Heise HM, Marbach R, Janatsch G, Kruse-Jarres JD (1989) Multivariate determination of glucose in whole blood by attenuated total reflection infrared spectroscopy. Anal Chem 61:2009–20015; erratum 67:775.

Hellberg S, Sjostrom M, Wold S (1986) The prediction of bradykinin potentiating potency of pentapeptides. An example of a peptide quantitative structure-activity relationship. Acta Chem Scand B 40:135–40.

Herscovitch P, Markham J, Raichle ME (1983) Brain blood flow measured with intravenous O-15 water: I. Theory and error analysis. J Nucl Med 24:782–789.

Hershenson M (1962) Reaction time as a measure of intersensory facilitation. J Exp Psychol 63:289–293.

Jenkins IH, Brooks DJ, Nixon PD, Frackowiak RSJ, Passingham RE (1994) Motor sequence learning: a study with positron emission tomography. J Neurosci 14:3775–3790.

Jueptner M, Frith CD, Brooks DJ, Frackowiak RS, Passingham RE (1997) Anatomy of motor learning. II. Subcortical structures and learning by trial and error. J Neurophysiol 77:1325–37.

Karni A, Meyer G, Jezzard P, Adams MM, Turner R, Ungerleider LG (1995) Functional MRI evidence for adult motor cortex plasticity during motor skill learning. Nature 377:155–158.

Lavond DG, Kim JJ, Thompson RF (1993) Mammalian brain substrates of aversive classical conditioning. Annu Rev Psychol 44:317–342.

Logan CG, Grafton ST (1995) Functional anatomy of human eyeblink conditioning determined with regional cerebral glucose metabolism and positron-emission tomography. Proc Natl Acad Sci USA 92:7500–7504.

Mackintosh NJ (1975) A theory of attention: variations in the associability of stimuli with reinforcement. Psychol Rev 82:276–298.

McGurk H, Macdonald J (1976) Hearing lips and seeing voices. Nature 264:746–748.

McIntosh AR, Gonzalez-Lima F (1994) Structural equation modeling and its application to network analysis in functional brain imaging. Hum Brain Mapp 2:2–22.

McIntosh AR, Bookstein FL, Haxby JV, Grady CL (1996a) Spatial pattern analysis of functional brain images using partial least squares. Neuroimage 3:143–157.

McIntosh AR, Grady CL, Haxby JV, Ungerleider LG, Horwitz B (1996b) Changes in limbic and prefrontal functional interactions in a working memory task for faces. Cereb Cortex 6:571–584.

Moeller JR, Strother SC, Sidtis JJ, Rottenberg DA (1987) Scaled subprofile model: a statistical approach to the analysis of functional patterns in positron emission tomographic data. J Cereb Blood Flow Metab 7:649–658.

Molchan SE, Sunderland T, McIntosh AR, Herscovitch P, Schreurs BG (1994) A functional anatomical study of associative learning in humans. Proc Natl Acad Sci USA 91:8122–8126.

Nyberg L, McIntosh AR, Cabeza R, Habib R, Houle S, Tulving E (1996a) Distinct brain regions involved in remembering what, where, and when. Proc Natl Acad Sci USA 93:11280–11285.

Nyberg L, McIntosh AR, Cabeza R, Nilsson L-G, Houle S, Habib R, Tulving E (1996b) Network analysis of positron emission tomography regional cerebral blood flow data: ensemble inhibition during episodic memory retrieval. J Neurosci 16:3753–3759.

Paus T, Petrides M, Evans A, Meyer E (1993) Role of the human anterior

cingulate in the control of oculomotor, manual, and speech responses: a positron emission tomography study. J Neurophysiol 70:453–469.

Pedhazur EJ (1982) Multiple regression in behavioral research: explanation and prediction. New York: Holt, Reinhart, and Winston.

Perruchet P (1985) Expectancy for airpuff and conditioned eyeblinks in humans. Acta Psychol 58:31–44.

Petrides M (1985) Deficits in associative-learning tasks after frontal- and temporal-lobe lesions in man. Neuropsychologia 23:601–614.

Petrides M, Pandya DN (1994) Comparative architectonic analysis of the human and the macaque frontal cortex. In: Handbook of neuropsychology (Boller F, Grafman J, eds), Vol. 9, pp. 17–57. Amsterdam: Elsevier.

Petrides M, Alivisatos B, Evans AC, Meyer E (1993) Dissociation of human mid-dorsolateral from posterior dorsolateral frontal cortex in memory processing. Proc Natl Acad Sci USA 90:873–877.

Recanzone GH, Schreiner CE, Merzenich MM (1992) Plasticity in the frequency representation of primary auditory cortex following discrimination training in adult owl monkeys. J Neurosci 13:87–103.

Sampson PD, Streissguth AP, Barr HM, Bookstein FL (1989) Neurobehavioral effects of prenatal alchohol: Part II. Partial least squares analysis. Neurotoxicol Teratol 11:477–491.

Schreurs BG, McIntosh AR, Bahron M, Herscovitch P, Sunderland T, Molchan SE (1997) Lateralization and behavioral correlation of changes in regional cerebral blood flow with classical conditioning of the human eyeblink response. J Neurophysiol 77:2153–2163.

Schultz W, Apicella P, Ljungberg T, Romo R, Scarnati E (1993) Reward-related activity in the monkey striatum and substantia nigra. Prog Brain Res 99:227–35.

Seitz RJ, Roland PE, Bohm C, Greitz T, Stone ES (1990) Motor learning in man: a positron emission tomographic study. NeuroReport 1:57–60.

Sekuler R and Sekuler A B. (1997) Sound alters visual-motion perception. Nature 385:308.

Stein B, Meredith M (1993) Merging of the senses. MIT Press: Cambridge, MA.

Stein BE, London N, Wilkinson LK, Price DD (1996) Enhancement of perceived visual intensity by auditory stimuli: a psychophysical analysis. J Cognit Neurosci 8:497–506.

Streissguth AP, Bookstein F, Sampson P, Barr H (1995) Attention: prenatal alcohol and continuities of vigilance and attentional problems from 4 through 14 years. Dev Psychopathol 7:419–446.

Streissguth AP, Bookstein FL, Sampson PD, Barr HM (1993) The enduring effects of prenatal alcohol exposure on child development: birth through seven years, a partial least squares solution. Ann Arbor, MI: University of Michigan Press.

Sutherland RW, Rudy JW (1989) Configuration association theory: the role of the hippocampal formation in learning, memory, and amnesia. Psychobiology 17:129–144.

Talairach J, Tournoux P (1988) Co-planar stereotaxic atlas of the human brain. New York: Thieme.

Weinberger NM, Diamond DM (1987) Physiological plasticity in auditory cortex: rapid induction by learning. Prog Neurobiol 29:1–55.

Wilson FA, Riches IP, Brown MW (1990) Hippocampus and medial temporal cortex: neuronal activity related to behavioural responses during the performance of memory tasks by primates. Behav Brain Res 40, 7–28.

Woods RP, Cherry SR, Mazziotta JC (1992) Rapid automated algorithm for aligning and reslicing PET images. J Comput Assist Tomogr 16:620–633.

Woody CD, Wang X-F, Gruen E, Landeira-Fernandez J (1992) Unit activity to click CS changes in dorsal cochlear nucleus after conditioning. NeuroReport 3:385–388.

Worsley K, Evans A, Marrett S, Neelin P (1992) A three-dimensional statistical analysis for CBF activation studies in human brain. J Cereb Blood Flow Metab 12:900–918.

Zhang J, Riehle A, Requin J, Kornblum S (1997) Dynamics of single neuron activity in monkey primary motor cortex related to sensorimotor transformation. J Neurosci 17:2227–2246.

Appendix

The algorithm for the design–brain–behavior (or multiblock) PLS analysis is different from the two-block case, in that the
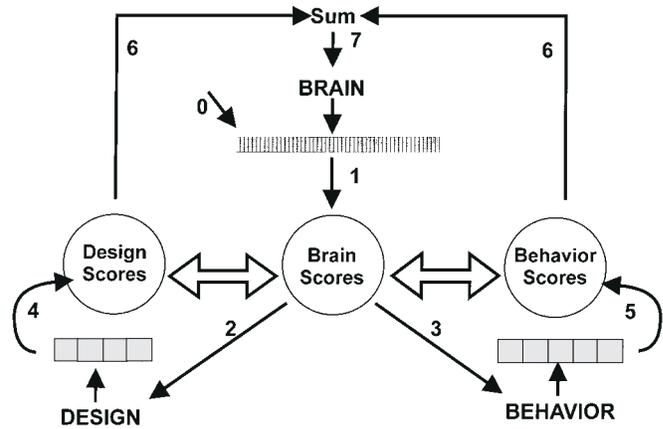

Figure A1. The algorithm for design–brain–behavior partial least squares analysis. Numbers 0–7 refer to steps of the algorithm (see Appendix for explanation).

multiblock algorithm is iterative, but the interpretation is essentially the same. Figure A1 shows the steps involved in the multiblock analysis. The bidirectional links in the middle of Figure A1 (open arrows) are consistent with a causal model that assumes the relation between design factors and behavior is mediated through the brain (i.e. no direct connection between design and behavior). The saliences (gray boxes) and scores can be estimated through the procedure outlined in Streissguth *et al.* (1993, pp. 77–81), which we briefly describe below. The procedure begins by assigning all voxels a salience of 1 (Fig. A1, step 0). The brain scores from these saliences are then computed (step 1). In steps 2 and 3, these brain scores are correlated with the design contrasts and behavior measures (within-task), yielding a tentative pattern of saliences for the design and behavior. Scores for these two blocks are computed in steps 4 and 5. In step 6, the tentative design and behavior LV scores are summed and then correlated with the raw image, resulting in a new set of saliences for the brain, and the cycle begins again. Convergence to a fixed point is assessed by examining changes in covariances among the three LV scores. The iterations continue until the change in the covariance between the design scores and brain scores, and brain scores and behavior scores is below some threshold.

The procedure depicted in Figure A1 is as follows:

After normalization of all variables to mean zero (not necessarily to variance 1), write X_i for the variables of the ith block (block 1 = design, block 2 = brain, block 3 = behavior). Write $cov(i,j)$ for the covariance matrix of the ith block with the jth block. LV_i indicates saliences for the latent variable of the ith block, and LVS_i for the latent variable scores of the ith block. The asterisk (*) denotes matrix multiplication. Then the algorithm is:

0. Initialize LV_2 to any arbitrary set of starting values (all 1's in the present case).
1. Compute scores $LVS_2 = X_2 * LV_2$.
2. Compute saliences $LV_i = cov(X_i, LV2)$, and scores $LVS_i = X_i * LV_i$, $i = 1,3$.
3. Update LV2 by $cov(LVS_1 + LVS_2, X_2)$.
4. Loop over (1)–(3) until the change in $cov(LV_i, LV_2)$ is stable to some preset tolerance.